ISSN 1674-1056
http://cpb.iphy.ac.cn
http://iopscience.iop.org/cpb
中国物理 B
Chinese Physics
中国物理 Chinese Physics B

Crystal structures and decomposing of B-P compounds under pressure

Die Zhang(张蝶), Xilian Jin(靳锡联), Quan Zhuang(庄全), Ying Li(李颖), Shuhan Yang(杨淑涵), Liying Song(宋丽莹), Bingbing Liu(刘冰冰), Tian Cui(崔田)

Citation: Chin. Phys. B . 2019, 28(5): 056101. **doi:** 10.1088/1674-1056/28/5/056101
Journal homepage: http://cpb.iphy.ac.cn; http://iopscience.iop.org/cpb

What follows is a list of articles you may be interested in

Function of large-volume high-pressure apparatus at SECUF

Pinwen Zhu(朱品文), Qiang Tao(陶强), Lu Wang(王璐), Zhi He(何志), Tian Cui(崔田)
Chin. Phys. B . 2018, 27(7): 076103. **doi:** 10.1088/1674-1056/27/7/076103

Compression behavior and phase transition of β-Si_3N_4 under high pressure

Hong-xia Gong(龚红霞), Zi-li Kou(寇自力), Cong Fan(樊聪), Hao Liang(梁浩), Qi-ming Wang(王齐明), Lei-lei Zhang(张雷雷), Fang Peng(彭放), Ming Yang(杨鸣), Xiao-lin Ni(倪小林), Jing Liu(刘景)
Chin. Phys. B . 2018, 27(5): 056101. **doi:** 10.1088/1674-1056/27/5/056101

Polycrystalline cubic boron nitride prepared with cubic-hexagonal boron nitride under high pressure and high temperature

Ming Yang(杨鸣), Zi-Li Kou(寇自力), Teng Liu(刘腾), Jing-Rui Lu(卢景瑞), Fang-Ming Liu(刘方明), Yin-Juan Liu(刘银娟), Lei Qi(戚磊), Wei Ding(丁未), Hong-Xia Gong(龚红霞), Xiao-Lin Ni(倪小林), Duan-Wei He(贺端威)
Chin. Phys. B . 2018, 27(5): 056105. **doi:** 10.1088/1674-1056/27/5/056105

Predicted novel insulating electride compound between alkali metals lithium and sodium under high pressure

Yang-Mei Chen(陈杨梅), Hua-Yun Geng(耿华运), Xiao-Zhen Yan(颜小珍), Zi-Wei Wang(王紫薇), Xiang-Rong Chen(陈向荣), Qiang Wu(吴强)
Chin. Phys. B . 2017, 26(5): 056102. **doi:** 10.1088/1674-1056/26/5/056102

Behaviors of Zn_2GeO_4 under high pressure and high temperature

Shu-Wen Yang(杨淑雯), Fang Peng(彭放), Wen-Tao Li(李文涛), Qi-Wei Hu(胡启威), Xiao-Zhi Yan(晏小智), Li Lei(雷力), Xiao-Dong Li(李晓东), Duan-Wei He(贺端威)
Chin. Phys. B . 2016, 25(7): 076101. **doi:** 10.1088/1674-1056/25/7/076101

Crystal structures and decomposing of B–P compounds under pressure*

Die Zhang(张蝶), Xilian Jin(靳锡联)†, Quan Zhuang(庄全), Ying Li(李颖), Shuhan Yang(杨淑涵), Liying Song(宋丽莹), Bingbing Liu(刘冰冰), and Tian Cui(崔田)‡

College of Physics, State Key Laboratory of Superhard Materials, Jilin University, Changchun 130012, *China*

(Received 15 November 2018; revised manuscript received 8 January 2019; published online 8 April 2019)

We have systematically studied the structures, electronic properties, and lattice dynamics of B–P compounds at high pressures. BP and B_6P are found to be thermodynamically stable below 100 GPa, and other stoichiometries are decomposable under pressure. The predicted structures of F-43m BP and R-3m B_6P are in good agreement with the experimental results by comparing the powder diffraction file (PDF) standard cards with our simulated x-ray diffractions. The bonding properties of BP and B_6P have also been analyzed by electronic localization functions, charge density difference, and Bader charge analysis. Our results show that BP and B_6P decompose into B and P under high pressure, which is proven to be dominated by the volumes of them. Furthermore, the infrared and Raman spectra of F-43m and R-3m are investigated at selected pressures and will provide useful information for future experimental studies about B–P compounds.

Keywords: B–P compounds, high pressure, structure

PACS: 61.50.Ah, 61.50.Ks, 61.66.Fn **DOI:** 10.1088/1674-1056/28/5/056101

1. Introduction

In the past few decades, the study of binary compounds under high pressure has attracted significant attention from scientists and researchers thanks to their potential excellent properties, such as high-temperature superconductivity, extreme hardness, and antimetallization.[1–8] Boride has been widely studied and applied in recent years. The cubic boron nitride (c-BN) shows excellent hardness, which is considered to be a promising superhard material in both technological and industrial applications.[9] A superconducting (SC) critical temperature T_c of 39 K has been observed in MgB_2.[10] Additionally, Fe_2B consisting of 99.97 wt% pure iron was found to provide excellent hardness and fracture toughness.[11] Titanium diboride has been applied in many fields due to some interesting properties, such as high melting point, excellent electrical conductivity, and thermal conductivity.[12]

Boron is a fascinating and complex element with only three valence electrons in the valence orbital, which is more likely to lose electrons and then become a common cation. In a room environment, pure boron and most of its compounds can be classified as insulators and semiconductors. Pressure can remarkably change the physical properties of materials and induce some unexpected and interesting physical phenomena. In the last few years, B has been widely investigated and was proposed to possess several fascinating structures, such as α-B_{12} (space group R-3m), β-B_{28} (space group $Pnnm$), and α-Ga (space group $Cmca$).[13,14] The phase of α-B_{12} icosahedron is close to β-B_{106} in terms of energy at ambient conditions, and becomes most competitive with pressure increasing until a more stable structure γ-B_{28} (28 atoms in the unit cell) emerges at 19 GPa.[14] The γ-B_{28} structure contains B_{12} icosahedron and B_2 pairs, which can be considered as "anions" and "cations", respectively.[14] A denser α-Ga phase of poor metallicity appears at 89 GPa and undergoes pressure-induced metal–insulator transitions above 300 GPa. Moreover, this phase is predicted to be superconductor with T_c value of 6 K at 175 GPa.[15] Phosphorus, which has five valence electrons per atom, shows a fascinating structural phase transition under pressure and exhibits some unique phases. Under ambient conditions, black P with $Cmca$ phase appears as a semiconductor structure and transforms into a semimetallic phase (R-3m) at 4.5 GPa. The R-3m phase undergoes a structural transition to a metallic SC phase (space group $Pm3m$) at 10 GPa and it is stable until 107 GPa.[16,17] Recently, superconductivity in the SC phase has been widely explored, and T_c value reaches 4.5–13 K under high pressure; however, the dependence of T_c on pressure remains controversial.[18,19] Then P transforms into the simple hexagonal phase of $P6/mmm$ at 132 GPa via an incommensurate modulation $Cmmm$,[20–22] and at higher pressure, another Im-3m phase becomes the most stable structure.[22] These interesting properties of B and P have aroused strong curiosity about exploring boron–

*Project supported by the National Natural Science Foundation of China (Grant Nos. 51632002, 51572108, 11634004, 11174102, and 11774119), the Program for Changjiang Scholars and Innovative Research Team in University, China (Grant No. IRT_15R23), the National Found for Fostering Talents of Basic Science, China (Grant No. J1103202), the National Key Research and Development Program of China (Grant No. 2016YFB0201204), the Development Program of Science and Technology of Jilin Province, China (Grant No. 20150312002ZG), and the 111 Project, China (Grant No. B12011).

†Corresponding author. E-mail: jinxilian@jlu.edu.cn

‡Corresponding author. E-mail: cuitian@jlu.edu.cn

© 2019 Chinese Physical Society and IOP Publishing Ltd

phosphorous under high pressure.

In recent decades, BP and B_6P have been investigated theoretically and experimentally. BP with F-43m structure can be synthesized experimentally from ambient environment to 110 GPa.[23] A recent theoretical study predicted that the zinc-blende structure transforms into rocksalt structure at 142 GPa.[24] The other theoretical result shows that the zincblende transforms to the nickel arsenide at 133.26 GPa, and then transforms to rocksalt at 211.99 GPa.[25] However, Zhang *et al.* reported that F-43m structure transforms to novel $C2/c$ structure at about 113 GPa and then changes to $P4_2/mnm$ above 208 GPa.[26] As for B_6P, a recent experiment on Raman about B_6P shows that the R-3m structure transforms to a distorted structure at 80 GPa.[27] In this work, we use the evolutionary local random structural prediction method along with first-principles calculations to investigate structures and properties of B–P compounds in the pressure range of 0–200 GPa. Only BP and B_6P compounds are thermodynamically stable under high pressures. Electronic properties, electronic band structures, bonding patterns, and dynamical stability of F-43m BP and R-3m B_6P are systematically investigated. Based on the experimental x-ray diffractions and theoretical simulations, we have proved the correctness of the structures we proposed. The infrared (IR) and Raman spectroscopies will provide reliable data for future scientific research about B–P compounds. Meanwhile, the decomposing mechanism of BP and B_6P is deeply analyzed.

2. Calculation methods

The structure prediction for B–P compounds at high pressures is performed by the in-house developed evolutional local random (ELocR) code.[28–30] The fully structural relaxation, electronic band structures, electronic localization functions (ELF), charge density difference, and Bader charge analysis are carried out by the Vienna *ab initio* simulation package (VASP).[31] We choose the Perdew–Burke–Ernzerhof (PBE) generalized gradient approximation (GGA) for the exchange–correlation function. The projector augmented wave (PAW) method is selected, s^2p^1 and s^2p^3 are considered as valence electrons for B and P, respectively. The plane-wave cutoff energy of 950 eV is adopted to ensure the convergence of total energy calculations. The electronic self-consistent calculation is stopped until the energy convergence is less than 10^{-6} eV.

Phonon calculations are carried out by a finite displacement approach through the Phonopy code.[32] The zero-point energy (ZPE) is obtained by

$$E_{\mathrm{ZPE}} = \frac{1}{2}\sum_{q\upsilon}\hbar\omega_{q\upsilon}, \tag{1}$$

where υ indicates a phonon branch at wave vector $\boldsymbol{q}$.

The Raman and IR spectra are calculated by Cambridge serial total energy package (CASTEP) code.[33] We use the PBE and GGA for the exchange–correlation function with norm-conserving pseudopotentials in the code, and the Brillouin zone sampling grid with a spacing of $2\pi\times0.03$ Å^{-1}.

To ensure the accuracy of our calculation, we have tested the convergence of energy cut-off and grid density, as shown in Fig. S1 in the Supplementary Material. The energy reaches convergence when the cut-off energy and grid density are 950 eV and $2\pi\times0.03$ Å^{-1} (i.e., the grid size of $16\times16\times16$ in the BP at 50 GPa in Fig. S1), respectively.

3. Results and discussions

Variable-composition structure searches for a variety of B–P stoichiometries are explored in the pressure range of 0–200 GPa. Whether these structures of different stoichiometries are thermodynamically stable depends on their formation enthalpies. The formation enthalpies ΔH_{f} is determined by the equation

$$\Delta H_{\mathrm{f}}(\mathrm{B}_x\mathrm{P}_y) = [H(\mathrm{B}_x\mathrm{P}_y) - xH(\mathrm{B}) - yH(\mathrm{P})]/(x+y), \tag{2}$$

where ΔH_{f} is the formation enthalpy per atom, and H is the calculated enthalpy per chemical unit for each compound. The ΔH_{f} values of B–P compounds with respect to solid B and P are shown in Fig. 1. BP and B_6P are thermodynamically stable below 100 GPa, while other stoichiometries lie above the decomposition line in the whole pressure range, indicating their thermodynamic instability.

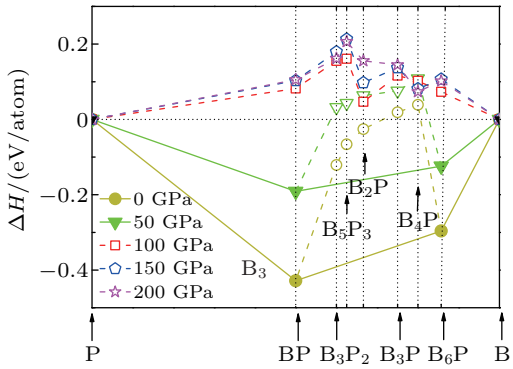


Fig. 1. Calculated formation enthalpies of B–P system with respect to B and P at selected pressures. Solid symbols (solid lines) represent the thermodynamically stable stoichiometries at corresponding pressures, and the open symbols (dashed lines) represent metastable ones.

The enthalpy–pressure curves of BP and B_6P are calculated in the range of 0–200 GPa. According to the enthalpy curves in Fig. 2(a), the cubic F-43m phase (Fig. 3(a)) is the most stable structure below 85 GPa. And the predicted phase is in good agreement with previous theoretical and experimental results.[34–36] In a recent theoretical study, $C2/m$ BP is proposed a stable metallic phase with a superconducting

critical temperature of 9.4 K–11.5 K at 113 GPa.[26] Unfortunately, $C2/m$ BP would be decomposed into B and P above 85 GPa based on our calculation of formation enthalpies. The enthalpy–pressure curves of several possible candidate structures of B_6P have also been explored. As shown in Fig. 2(b), the trigonal structure of R-3m (Fig. 3(b)) which is proposed by Guo *et al*,[37] is stable below 81.4 GPa. The boron icosahedron is discovered in the R-3m structure and connects with P atoms. In the icosahedron, three B atoms are located in the upper part, three B atoms are in the lower part, and the other six equivalent B atoms form the middle part. The structural information for F-43m and R-3m phases are summarized in Table S1. Using the radiational wavelengths of 1.542 Å and 1.789 Å, the x-ray diffraction (XRD) patterns of the predicted BP and B_6P are simulated and compared with powder diffraction file (PDF) standard card at ambient pressure. As shown in Fig. S2, the calculated XRD patterns agree well with the PDF standard card.

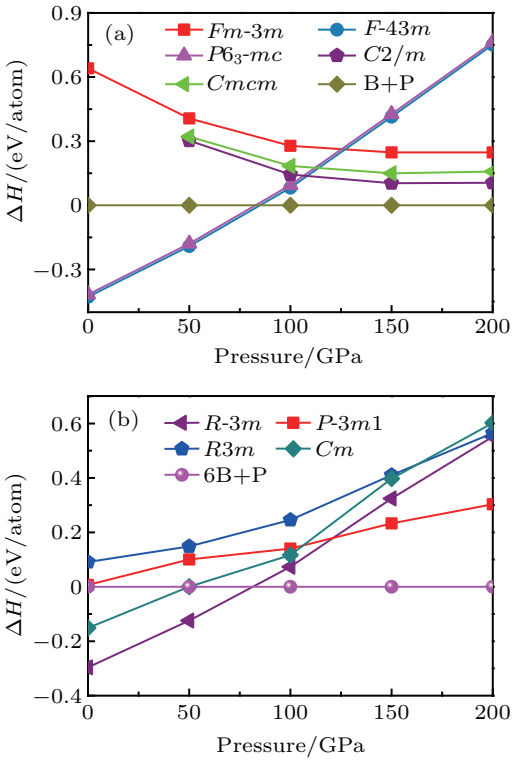


Fig. 2. Calculated enthalpies per atom as a function of pressure. The formation enthalpies of (a) BP and (b) B_6P are shown relative to the decomposition to B+P and 6B+P, respectively.

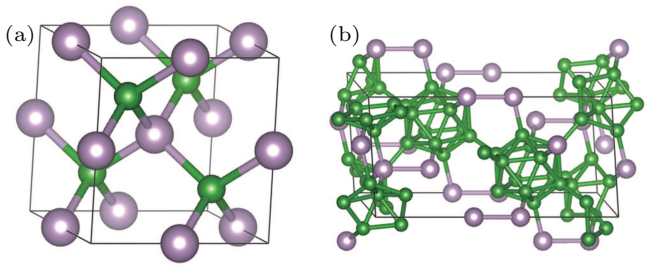


Fig. 3. Crystal structures of (a) F-43m BP and (b) R-3m B_6P at 40 GPa. Purple and green spheres depict P and B atoms, respectively.

The properties of decomposing B–P compounds were then explored by analyzing the formation enthalpies. The different enthalpy curves of B_6P, BP+5B, and 6B+P at 0–200 GPa are displayed in Fig. 4. B_6P is thermodynamically unstable and decomposes into BP and B mixtures above 81.4 GPa, and BP completely becomes B and P mixtures at 85 GPa. Generally, BP and B_6P are thermodynamically stable in lower pressure range, and decompose into B and P at higher pressures. It is necessary to consider the ZPE in B–P compounds due to the lighter elements of B.[38] Considering the ZPEs of BP, B_6P, B, and P with the harmonic approximation, the shift of decomposition pressure to lower pressures can be found in Fig. S3, i.e., from 85 GPa to 82.8 GPa for BP and 81.4 GPa to 80.1 GPa for B_6P, respectively.

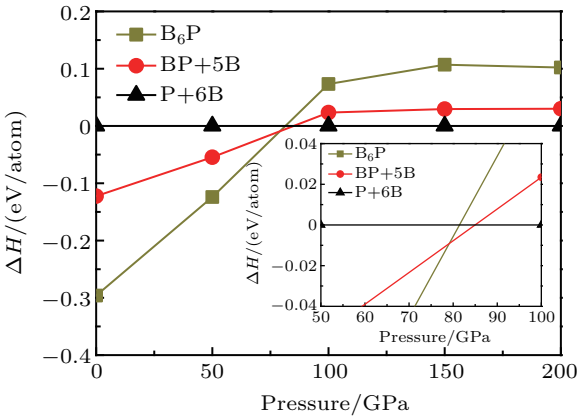


Fig. 4. The formation enthalpies of B_6P and BP+5B relative to the decomposition to 6B+P in the pressure range of 0–200 GPa. The inset exhibits ΔH in the 50–100 GPa.

We then analyze the structural decomposing of BP and B_6P under high pressures. Enthalpy has two parts: the product of pressure and volume PV, and the internal energy U. The following formulas are adopted to quantify the difference of V and U of BP and B_6P relative to the decomposition products B and P:

$$P\Delta V(\mathrm{B}_x\mathrm{P}) = P[V(\mathrm{B}_x\mathrm{P}) - xV(\mathrm{B}) - V(\mathrm{P})], \quad (3)$$

$$\Delta U(\mathrm{B}_x\mathrm{P}) = [U(\mathrm{B}_x\mathrm{P}) - xU(\mathrm{B}) - U(\mathrm{P})], \quad (4)$$

where x is 1 for BP and 6 for B_6P. The calculated information about decomposing of B–P compounds is shown in Figs. 5(a) and 5(b). Meanwhile, the pressure dependence of crystal volumes in BP, B_6P, B, and P is displayed in Figs. 5(c) and 5(d). The volume change can be quantified by

$$\Delta V_{\mathrm{BP}} = V(\mathrm{BP}) - V(\mathrm{B}) - V(\mathrm{P}), \quad (5)$$

$$\Delta V_{\mathrm{B_6P}} = V(\mathrm{B_6P}) - 6V(\mathrm{B}) - V(\mathrm{P}). \quad (6)$$

As shown in Fig. 5 and Table 1, both BP and B_6P are thermodynamically stable below 14.4 GPa and 8.2 GPa, respectively. And the volumes of them are much smaller than that of the decomposition products of B and P. Although the volumes of BP and B_6P decrease as the pressure increases, the

ΔV_{BP} and ΔV_{B_6P} rise gradually and play a more important role on stability than that in lower pressure range. At the intersection points—i.e., 14.4 GPa and 8.2 GPa in Figs. 5(c) and 5(d)—the compounds of BP and B_6P have the same volume as the decomposition products of B and P. However, the compounds of BP and B_6P are more stable than the decomposition products of B and P because the internal energy contributes more to thermodynamic stability than that of volume. After the intersection points of pressures, the contribution of volume gradually increases; meanwhile, the contribution from internal energy decreases with pressure, see Table 1. Two competing aspects of internal energy and volume are in equilibrium at the pressures of 85 GPa for BP and 81.4 GPa for B_6P, respectively, and the decompositions from the compounds to B and P will occur at the same pressures. Above equilibrium pressure, the contribution from the volume is greater than that of internal energy and results in the decompositions of compounds of BP and B_6P, as shown in Table 1 and Fig. 5.

Meeting the mechanical stability is a fundamental condition for a stable crystal structure, and the elastic constant matrix should be positive depending on Boron–Huang mechanical stability.[39] The calculated elastic constant matrix C_{ij} of BP and B_6P at selected pressures are listed in Table S2. For cubic structure of F-43m BP, it satisfies these inequalities: $C_{11} > 0$, $C_{44} > 0$, $C_{11} > |C_{12}|$, and $C_{11} + 2C_{12} > 0$, indicating the mechanical stable property.[40] For R-3m B_6P, it also satisfies the inequalities: $C_{44} > 0$, $C_{11} > |C_{12}|$, and $(C_{11} + 2C_{12})C_{33} > 2C_{13}^2$. Therefore, the F-43m BP and R-3m B_6P are mechanically stable at corresponding pressures.[40]

Table 1. The calculated contributions of ΔU and $P\Delta V$ to thermodynamic stability of BP and B_6P at different pressures.

	0 GPa	20 GPa	40 GPa	60 GPa	80 GPa	100 GPa
BP (ΔU)	100.0%	80.0%	67.5%	58.5%	51.7%	46.3%
BP ($P\Delta V$)	0.0%	20.0%	32.5%	41.5%	48.3%	53.7%
B_6P (ΔU)	100.0%	79.6%	66.9%	57.9%	51.1%	46.1%
B_6P ($P\Delta V$)	0%	20.4%	33.1%	42.1%	48.9%	53.9%

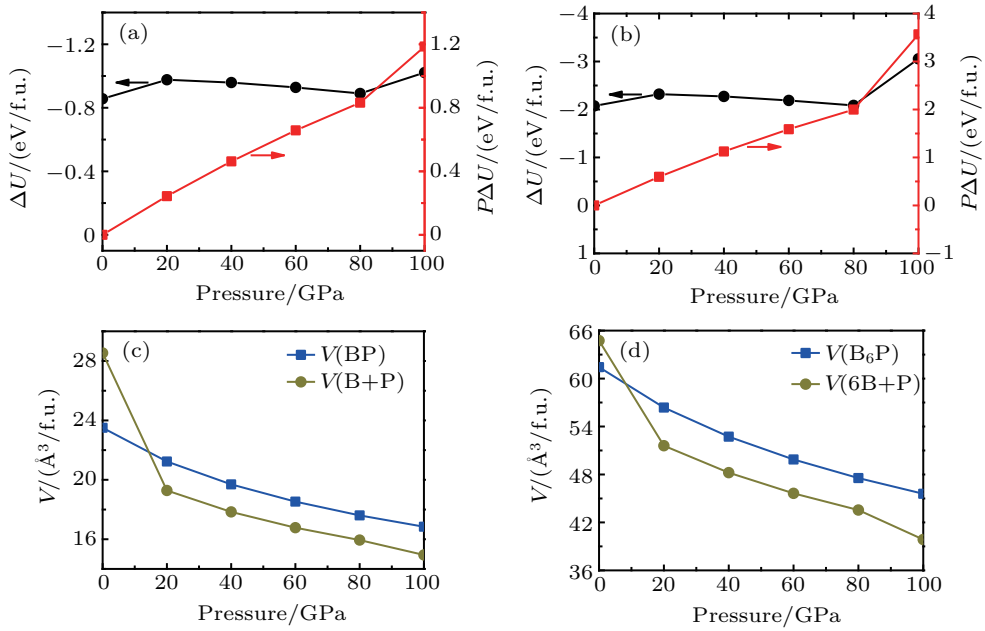


Fig. 5. The calculated product of pressure and volume PV and the internal energy U of BP and B_6P with respect to B and P as a function of pressure. (a) The $P\Delta V$ and ΔU of BP; (b) the $P\Delta V$ and ΔU of B_6P; (c) and (d) the calculated volume per BP and B_6P with respect to the decomposition to B+P and 6B+P at corresponding pressures.

We have also evaluated the hardness of BP and B_6P with the equation

$$H_v = 2\left(k^2 G\right)^{0.585} - 3, \tag{7}$$

where k indicates a Pugh's modulus ratio, and can be expressed as $k = G/B$.[41]

The hardness of B_6P is 42.3 GPa at ambient pressure, and it is a potential superhard material with H_v higher than 40 GPa. For BP, which is the same group boride as the c-BN, it is also crystallized in cubic crystal; however, the H_v of BP is 36.1 GPa, which is smaller than the value of 40.9 GPa in c-BN. The calculated Pugh's ratios of BP and c-BN are 0.99 and 0.79, and the G values are 162.28 for BP and 315 for c-BN,[42] respectively. The difference of H_v is attributed to the shear modulus G.

To determine the dynamical stability of the crystal struc-

ture, we have calculated the phonon band structure and projected phonon density of states (PHDOS) of BP and B_6P at selected pressures, as shown in Fig. 6. At 0 GPa and 40 GPa, both structures demonstrate their dynamical stability without negative frequency in the entire Brillouin zone. From Figs. 6(a) and 6(b), we can see that the low frequency modes mainly come from the vibrations of P atoms, and the higher frequency modes are mainly associated with B atoms due to the heavier atomic mass of P than that of B. Due to the higher content of atoms of B than that of P in the unit cell of *R*-3*m* B_6P, the contribution to vibration modes mainly comes from B atoms (Figs. 6(c) and 6(d)). With the pressure increasing, the phonon modes tend to harden in both *F*-43*m* BP and *R*-3*m* B_6P.

Raman spectra, which provide important information in the research of crystal structures and bonding properties, are simulated and compared with experimental results for BP and B_6P. For *R*-3*m* B_6P phase, the Raman active frequency of our theoretical calculation is in good agreement with previous experimental result at 0 GPa.[27] With the pressure increasing, B_6P shows an expected phenomenon of a hardening of almost all the Raman modes, and a Raman mode ascending to a very high frequency of 1438.83 cm^{-1} at 80 GPa. There is no Raman mode below 200 cm^{-1} [27] till the decomposition of B_6P compound. For the *F*-43*m* BP, there is only a Raman mode of 781.30 cm^{-1} at atmospheric pressure, which is slightly lower than 794 cm^{-1} and 823 cm^{-1} by Vladimir *et al.*[16] The relationship between Raman mode and pressure is depicted in Fig. S4. The Raman peak of *F*-43*m* phase tends to a higher frequency due to the shrinkage of B–P bond as the pressure increases. Our calculation is consistent with Vladimir's experimental result on the evolution of Raman shift with pressures.[16] Furthermore, the vibrational modes of IR and Raman on the phases of *F*-43*m* BP and *R*-3*m* B_6P can be classified by the irreducible representation of the point groups T_d and D_{3d}, as shown in Table S3. There are two atoms in the primitive cell of the *F*-43*m* structure; therefore, six vibrational modes are produced including three optical modes $3T_2$ which are third-degree degeneration. So $\Gamma_{optic} = 3T_2$, and T_2 mode is both IR active and Raman active. In *R*-3*m* phase, there are 14 atoms in the primitive cell, and therefore, there are 42 vibrational modes including 39 optical modes, arrived at $\Gamma_{optic} = 2A_{1u} + 4A_{2u} + 12E_u + 14E_g + 5A_{1g} + 2A_{2g}$. The A_{2u} and E_u modes are IR active; E_g and A_{1g} modes are Raman active; A_{1u} and A_{2g} are silent; E_u and E_g are second-degree degeneration.

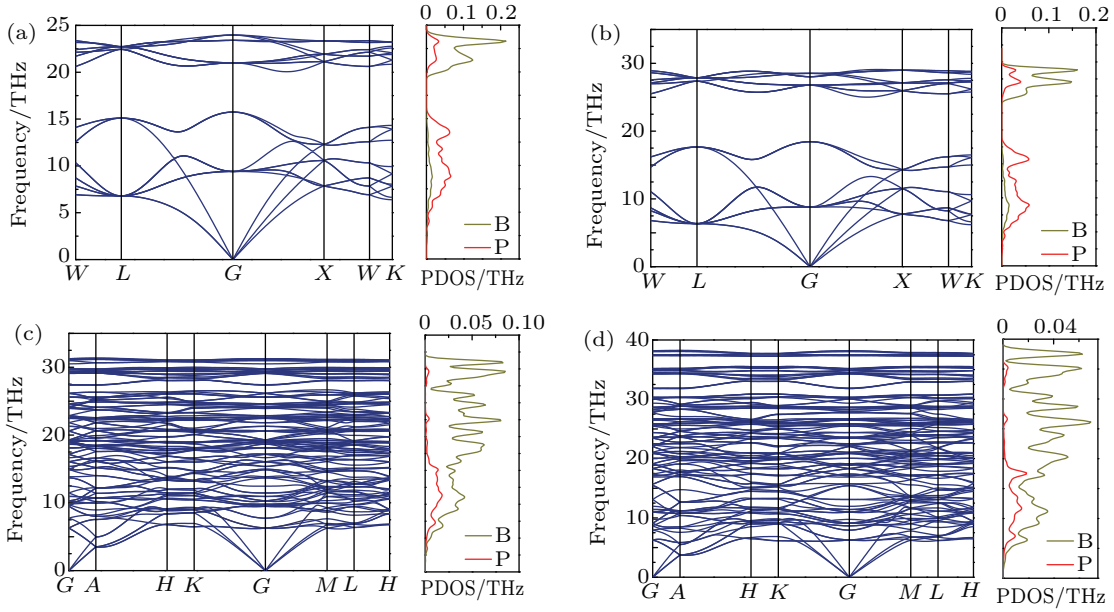


Fig. 6. Phonon dispersions and projected phonon density of states for (a) *F*-43*m* BP at 0 GPa, (b) *F*-43*m* BP at 40 GPa, (c) *R*-3*m* B_6P at 0 GPa, and (d) *R*-3*m* B_6P at 40 GPa.

In the meantime, the electronic properties of BP and B_6P are calculated. The band structures of BP and B_6P near Fermi energy at high pressure are shown in Fig. S5. Obviously, BP and B_6P are indirect bandgap semiconductors, with the feature that the maximum value of the valence band and the minimum value of conduction band are not on the same high symmetry point. The electron localization function and charge density difference are calculated to investigate the bonding characteristics and distribution of electrons in B–P compounds. The ELF of 1 represents electron complete localization, the ELF of 0.5 reflects the probable electron-gas-like pairs, and the value of 0 expresses non-electron localization. Figures S6(a) and S6(b) disclose three dimensional ELFs for *F*-43*m* BP and *R*-3*m* B_6P at 40 GPa with an isosurface value of 0.75, respectively. Apparently, a large number of valence electrons accumulate in the interstitial regions of both crystals. According to

Figs. S6(c) and S6(d), the valence electrons are localized between B and P atoms, indicating that B and P have strong covalent interaction for F-43m phase. Meanwhile, valence electrons are found to localize between the neighbouring B atoms and P atoms in R-3m. In R-3m phase, there are two kinds of B–B bonds, one is located on the boron icosahedra surface (B–B^1) and the other connects the icosahedra (B–B^2). The ELF value of B–B^1 bond reaches 0.84, which is much smaller than the value of 0.97 of the B–B^2 bond. In addition, the ELF values of the B–P and P–P bond are 0.96 and 0.93, respectively. The value of ELF around the outside of boron icosahedra is much larger than that on the surface of boron icosahedra. The relationship between the ELF values and pressure for all bonds of B–P compounds is shown in Table S4. Additionally, in the F-43m structure at 0 GPa, Bader charge analysis discloses the charge transfer from B to P. Due to the variety of bonds in R-3m B_6P, the result based on Bader charge analysis becomes complex. Although the total charge transfer from B to P can be found in R-3m phase, the transfers of B→B and P→P are also observed here, as shown in Table S5.

4. Conclusion

In summary, we have executed systematic searching for crystal structures of B–P system in the pressure range of 0–200 GPa by utilizing evolutionary structure searches. Two stoichiometries of BP and B_6P are discovered to be thermodynamically stable below 85 GPa and 81.4 GPa, respectively. The electronic energy band structures demonstrate that both BP and B_6P are indirect bandgap semiconductors at corresponding pressure interval. The analyses of ELF display the complicated bonding characteristic of BP and B_6P. With further investigation of IR and Raman spectra of BP and B_6P, we have observed that BP and B_6P express a phenomenon with a hardening of all the Raman modes. Accurate vibrational modes are helpful in further experimental study about interesting phenomena of B–P compounds at high pressures. The analyses of decomposing mechanism of BP and B_6P show that the decomposing of BP and B_6P is dominated by the volumes of B, P, and corresponding B–P compounds. Less-packed BP and B_6P would be more likely to be thermodynamically unstable under high pressure. In addition, our conclusions will provide a great push to research to explore the structures and properties of other borides.

Acknowledgment

Parts of the calculations were performed in the High Performance Computing Center (HPCC) of Jilin University.

References

[1] Wang Z W, Yao Y S, Zhu L, Liu H Y, Iitaka T, Wang H and Ma Y M 2014 *J. Chem. Phys.* **140** 124707
[2] Lu C, Li Q, Ma Y M and Chen C F 2017 *Phys. Rev. Lett.* **119** 115503
[3] Howie R T, Guillaume C L, Scheler T, Goncharov A F and Gregoryanz E 2012 *Phys. Rev. Lett.* **108** 125501
[4] Drozdov A P, Eremets M I, Troyan I A, Ksenofontov V and Shylin S I 2015 *Nature* **525** 73
[5] Jin X L, Chen X J, Cui T, Mao H K, Zhang H D, Zhuang Q, Bao K, Zhou D W, Liu B B, Zhou Q and He Z 2016 *Proc. Natl. Acad. Sci. USA* **113** 2366
[6] Zhuang Q, Jin X L, Cui T, Zhang D, Li Y, Li X, Bao K and Liu B B 2018 *Phys. Rev. B* **98** 024514
[7] Jin X L, Meng X, He Z, Ma Y M, Liu B B, Cui T, Zou G T and Mao H K 2010 *Proc. Natl. Acad. Sci. USA* **107** 9969
[8] Yuan Y F, Zhang Z T, Wang W K, Zhou Y H, Chen X L, An C, Zhang R R, Zhou Y, Gun C C, Li L, Li X J and Yang Z R 2018 *Chin. Phys. B* **27** 066201
[9] Zheng J C 2005 *Phys. Rev. B* **72** 052105
[10] Larbalestier D C, Cooley L D, Rikel M O, *et al.* 2001 *Nature* **410** 186
[11] Ozdemir O, Usta M, Bindal C and Ucisik A H 2006 *Vacuum* **80** 1391
[12] Peng F, Fu H Z and Cheng X L 2007 *Phys. B* **400** 83
[13] Lazzari R, Vast N, Besson J M, Baroni S and Corso A D 1999 *Phys. Rev. Lett.* **83** 3230
[14] Oganov A R, Chen J H, Gatti C, Ma Y Z, Ma Y M, Glass C W, Liu Z X, Yu T, Kurakevych O O and Solozhenko V L 2009 *Nature* **457** 863
[15] Häussermann U, Simak S I, Ahuja R and Johansson B 2003 *Phys. Rev. Lett.* **90** 065701
[16] Solozhenko V L, Kurakevych O O, Godec Y L, Kurnosov A V and Oganov A R 2014 *J. Appl. Phys.* **116** 033501
[17] Jamieson J C 1963 *Science* **139** 1291
[18] Chan K T, Malone B D and Cohen M L 2013 *Phys. Rev. B* **88** 064517
[19] Kawamura H, Shirotani I and Tachikawa K 1985 *Solid State Commun.* **54** 775
[20] Fujihisa H, Akahama Y, Kawamura H, Ohishi Y, Gotoh Y, Yamawaki H, Sakashita M, Takeya S and Honda K 2007 *Phys. Rev. Lett.* **98** 175501
[21] Akahama Y, Kobayashi M and Kawamura H 1999 *Phys. Rev. B* **59** 8520
[22] Akahama Y, Kawamura H, Carlson S, Bihan T L and Häussermann D 2000 *Phys. Rev. B* **61** 3139
[23] Xia H, Xia Q and Ruoff A L 1993 *J. Appl. Phys.* **74** 1660
[24] Cui S X, Feng W X, Hu H Q, Feng Z B and Wang Y X 2009 *Comput. Mater. Sci.* **44** 1386
[25] Arbouche O, Belgoumène B, Soudini B, Azzaz Y, Bendaoud H and Amara K 2010 *Comput. Mater. Sci.* **47** 685
[26] Zhang X Y, Qin J Q, Liu H Y, Zhang S L, Ma M Z, Luo W, Liu R P and Ahuja R 2015 *Sci. Rep.* **5** 8761
[27] Ovsyannikov S V, Polian A, Munsch P, Chervin J C, Marchand G L and Aselage T L 2010 *Phys. Rev. B* **81** 140103(R)
[28] Li Y, Jin X L, Cui T, Zhuang Q, Lv Q Q, Wu G, Meng X, Bao K, Liu B B and Zhou Q 2017 *RSC Adv.* **7** 7424
[29] Zhuang Q, Jin X L, Lv Q Q, Li Y, Shao Z J, Liu Z, Li X, Zhang H D, Meng X, Bao K and Cui T 2017 *Phys. Chem. Chem. Phys.* **19** 26280
[30] Lv Q Q, Jin X L, Cui T, Zhuang Q, Li Y, Wang Y C, Bao K and Meng X 2017 *Chin. Phys. B* **26** 076103
[31] Kresse G and Furthmüller J 1996 *Phys. Rev. B* **54** 11169
[32] Togo A, Oba F and Tanaka I 2008 *Phys. Rev. B* **78** 134106
[33] Clark S J, Segall M D, Pickard C J, Hasnip P J, Probert M J, Refson K and Payne M C 2005 *Z. Kristallogr.* **220** 567
[34] Wentzcovitch R M, Chang K J and Cohen M L 1986 *Phys. Rev. B* **34** 1071
[35] Zaoui A and Hassan F E H 2001 *J. Phys.: Condens. Matter* **13** 253
[36] Mukhanov V A, Sokolov P S, Godec Y L and Solozhenko V L 2013 *J. Superhard Mater.* **35** 415
[37] Guo X J, He J L, Liu Z Y, Tian Y J, Sun J and Wang H T 2006 *Phys. Rev. B* **73** 104115
[38] van Setten M J, Uijttewaal M A, de Wijs G A and de Groot R A 2007 *J. Am. Chem. Soc.* **129** 2458
[39] Robertson J H 1985 *Acta Crystallogr. Sect. A* **41** 624
[40] Wu Z J, Zhao E J, Xiang H P, Hao X F, Liu X J and Meng J 2007 *Phys. Rev. B* **76** 054115
[41] Chen X Q, Niu H Y, Li D Z and Li Y Y 2011 *Intermetallics* **19** 1275
[42] Grimsditch M, Zouboulis E S and Polian A 1994 *J. Appl. Phys.* **76** 832